ELSEVIER

Ceramics International 30 (2004) 2223–2227

CERAMICS INTERNATIONAL

www.elsevier.com/locate/ceramint

Effect of polyethylene glycol on the microstructure and PTCR characteristics of *n*-$BaTiO_3$ ceramics

Jun-Gyu Kim [a,*], Weon-Pil Tai [a], Ki-Ju Lee [b], Won-Seung Cho [b]

[a] *Institute of Advanced Materials, Inha University, Inchon 402-751, Republic of Korea*
[b] *School of Materials Science and Engineering, Inha University, Inchon 402-751, Republic of Korea*

Received 17 December 2003; received in revised form 9 January 2004; accepted 5 February 2004
Available online 20 April 2004

Abstract

Porous $BaTiO_3$ (*n*-$BaTiO_3$) ceramics doped donor were fabricated by the addition of polyethylene glycol (PEG) into the *n*-$BaTiO_3$ powder. The effects of PEG on the microstructure and PTCR characteristics of the porous *n*-$BaTiO_3$ ceramics have been investigated. An endotherm was found at 60 °C, with strong exotherm at 262 °C, weight loss commenced at 165 °C and was virtually complete by 265 °C from the differential thermal analysis (DTA) and thermogravimetric analysis (TGA) of the PEG. It was also found that the porosity increased and the grain size decreased with increasing PEG. The crystalline structure of *n*-$BaTiO_3$ ceramics was independent on the PEG content and the *n*-$BaTiO_3$ ceramics containing PEG showed the presence of (Ba, Sr)TiO_3 peaks only from the XRD results. The *n*-$BaTiO_3$ ceramics containing PEG showed higher PTCR characteristics than that of the *n*-$BaTiO_3$ ceramics without PEG.

Keywords: Porous *n*-$BaTiO_3$ ceramics; PTCR; Polyethylene glycol

1. Introduction

Donor doped $BaTiO_3$ (*n*-$BaTiO_3$) ceramics exhibit a positive temperature coefficient of resistivity (PTCR) [1–11]. A widely accepted model that elucidates the conduction mechanism of the PTCR characteristic has been proposed by Heywang [8]. PTCR characteristics originate from the existence of an electrical potential barrier arising from the presence of a two-dimensional surface layer of acceptor states, e.g., segregated acceptor ions, or adsorbed oxygen at the grain boundaries [8–13].

The transition temperature, which is near the ferroelectric Curie point (T_c), shifts to lower temperature upon substitution of Sr^{2+} for Ba^{2+}. The PTCR thermistors are used in a variety of applications, including current limiting and thermal controllers. Various fabrication techniques have been attempted to investigate the PTCR characteristic and improve the thermistors performance [12,13].

It has been reported that porous *n*-$BaTiO_3$ exhibited large PTCR characteristics [14–16]. Oxygen can be adsorbed at the grain boundaries due to the presence of pores in the porous ceramics, which are more favorable to form surface acceptor states compared with ordinary dense ceramics [13]. Porous *n*-$BaTiO_3$ has been fabricated by the incorporation of graphite, borides, silicides, carbides, partially oxidized Ti powder, corn- and potato-starch to $BaTiO_3$ [14–18].

In this study, porous *n*-$BaTiO_3$ ceramics are prepared by adding polyethylene glycol (PEG). The PEG utilized pore-forming agent is a very cheap material compared with the above-mentioned additives. The effects of PEG on the microstructure and electrical properties were carefully investigated.

2. Experimental procedure

High-purity $BaTiO_3$ ceramic powder was utilized in this study (Toho Titanium Co. Ltd., Japan). The powder was commercially obtained as $BaTiO_3$ powder containing $SrTiO_3$ (19.2 mol%) and Y_2O_3 (0.2 mol%). The mean particle size and ferroelectric Curie temperature of the powder were 0.7 μm and 61 °C, respectively. The PEG (powder form, mean particle size: 50 μm, Shinyo Pure Chemicals Co. Ltd., Japan), with amount ranging from 1 to 20 wt.% was added to the *n*-$BaTiO_3$ powder and then mixed in

* Corresponding author.
E-mail address: jgkim@munhak.inha.ac.kr (J.-G. Kim).

0272-8842/$30.00 © 2004 Elsevier Ltd and Techna S.r.l. All rights reserved.
doi:10.1016/j.ceramint.2004.02.001

a mortar for 1 h. The mixed powder were compacted by die-pressing at a pressure of 40 MPa to prepare the green compacts (15 mm × 12 mm × 7 mm). The green compacts were sintered at 1350 °C for 1 h in air. The samples were heated up to the sintering temperature at a rate of 3 °C/min, and cooled at a rate of 10 °C/min from the sintering temperature to 300 °C, and then furnace cooled.

Both faces of the samples (15 mm × 12 mm) were contacted with ohmic electrodes. The commercial ohmic paste (Ag–7 mass% Ni) of ~10 μm thickness was thinly spread on the two sides of the surfaces. After the paste was dried at room temperature, the Ag paste of ~10 μm thickness was covered on the ohmic paste layers. These pastes were baked at 580 °C for 5 min with a heating rate of 10 °C/min in air.

The microstructure, phase identification and crystalline structure of the *n*-$BaTiO_3$ ceramics were analyzed by scanning electron microscopy (SEM: S-4200, Hitachi) and X-ray diffraction (XRD: PW-1710, Philips, Cu), respectively. The average grain size of the ceramics was estimated by the line-intersection method. The electrical resistance was measured with a digital multi-meter under air atmosphere. In order to determine the separate electrical properties of grain boundary and grain, complex impedance analysis was conducted with an impedance analyzer (HP LF 4192A) at room temperature and 150 °C in the frequency range of 5 Hz–13 MHz. Differential thermal analysis (DTA) and thermogravimetric analysis (TGA) of the PEG was performed in air, at a heating rate of 10 °C/min, using a Thermal Analyzer (SDT Q600).

3. Results and discussion

DTA and TGA were performed on the PEG material used as additive. The result is illustrated in Fig. 1. An endotherm was found at 60 °C, with strong exotherm at 262 °C. Weight loss commenced at 165 °C and was virtually complete by 265 °C. It was found that no residue was found after heating PEG to 300 °C.

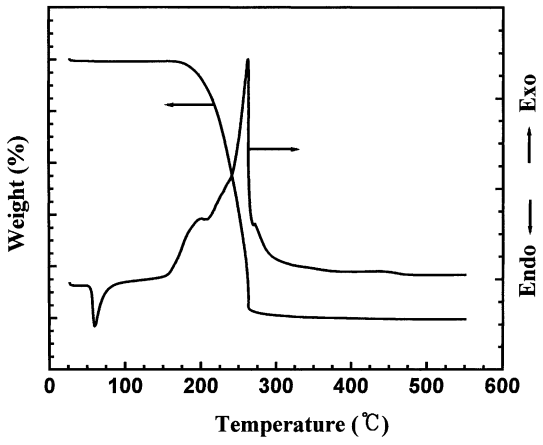

Fig. 1. DTA–TGA curves of PEG.

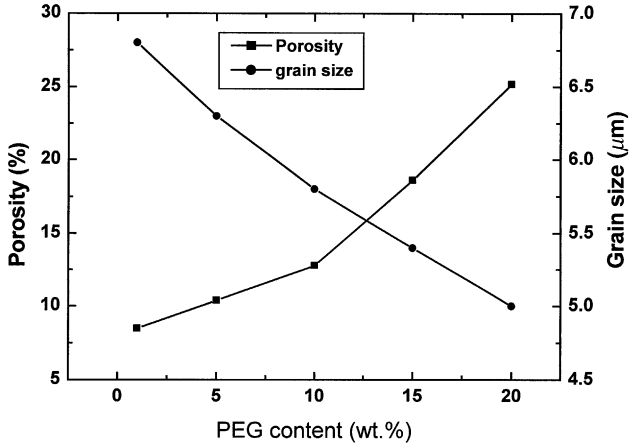

Fig. 2. Porosity and grain size of the *n*-$BaTiO_3$ ceramics containing various amount of PEG.

Fig. 2 shows the porosity and grain size of *n*-$BaTiO_3$ ceramics containing various amount of PEG. The porosity increased and the grain size decreased with increasing PEG content. For example, the porosity and grain size of the *n*-$BaTiO_3$ ceramic containing 5 wt.% PEG is 10.4% and 6.3 μm, respectively, while it is 25.2% and 5.0 μm, respectively for the *n*-$BaTiO_3$ ceramic containing 20 wt.% PEG. These porous ceramics are advantageous to oxidize grain boundaries and to produce surface acceptor states [9]. The porosity of the *n*-$BaTiO_3$ ceramics containing the PEG increased with increasing PEG content. This can be explained by the fact that the cavities formed due to the burning-out of PEG during sintering act as the sites of the pore generation.

Fig. 3 shows the SEM micrographs of the fractured surfaces for the *n*-$BaTiO_3$ ceramics containing (a) 5 wt.%, (b) 15 wt.% and (c) 20 wt.% of PEG. It is confirmed that the porosity increased and the grain size decreased with increasing PEG content.

The phases present in the *n*-$BaTiO_3$ ceramics without and with PEG were confirmed by XRD as shown in Fig. 4. This figure shows the presence of (Ba, Sr)TiO_3 peaks only in the *n*-$BaTiO_3$ ceramics with and without PEG.

Also, in order to investigate the effect of PEG content on the crystalline structure, XRD analysis was performed with the *n*-$BaTiO_3$ ceramics containing PEG. Fig. 5 shows the XRD patterns measured at room temperature for *n*-$BaTiO_3$ ceramics containing (a) 0 wt.%, (b) 10 wt.% and (c) 20 wt.% of PEG. It is difficult to identify the tetragonal and cubic phases in (Ba, Sr)TiO_3, since the lattice parameters of the two phases are quite similar. The crystalline structure of the two phases was thus analyzed at high angles. Fig. 5 shows the (1 0 3) and (3 1 0) peaks of the tetragonal phases. The *n*-$BaTiO_3$ ceramics without PEG (Fig. 5a) had the tetragonal structure and all the *n*-$BaTiO_3$ ceramics containing PEG including the samples containing 10 and 20 wt.% PEG (Fig. 5b and c) also had the tetragonal structure. This suggests that the crystalline structure of the *n*-$BaTiO_3$ ceramics at room temperature is independent on the PEG content.

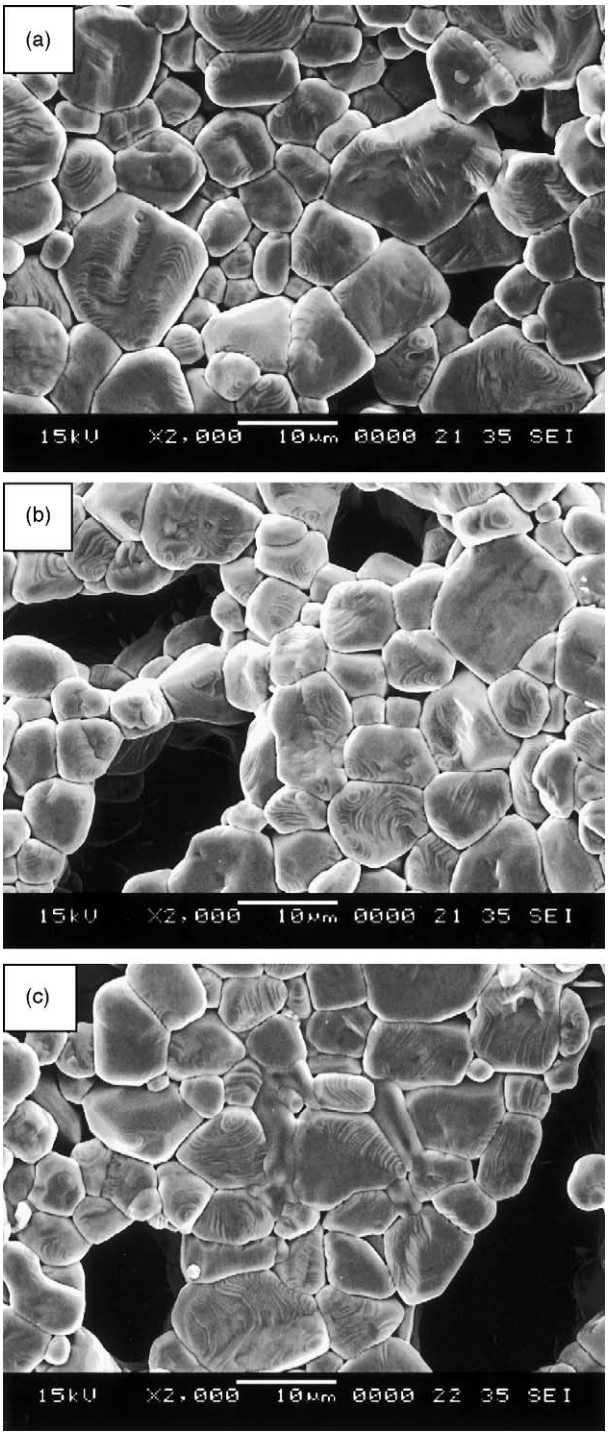

Fig. 3. SEM micrographs of the fractured surfaces for the n-$BaTiO_3$ ceramics containing (a) 5 wt.%, (b) 15 wt.% and (c) 20 wt.% PEG.

Fig. 6 shows the effect of temperature on the electrical resistivity of the n-$BaTiO_3$ ceramics containing various amount of PEG. All the n-$BaTiO_3$ ceramics showed PTCR behavior in which the PTCR jump was slightly increased with increasing PEG content. For example, the PTCR jump of the n-$BaTiO_3$ ceramics containing PEG of 1 and 20 wt.% is 2.84×10^5, 6.76×10^5, respectively. The enhancement

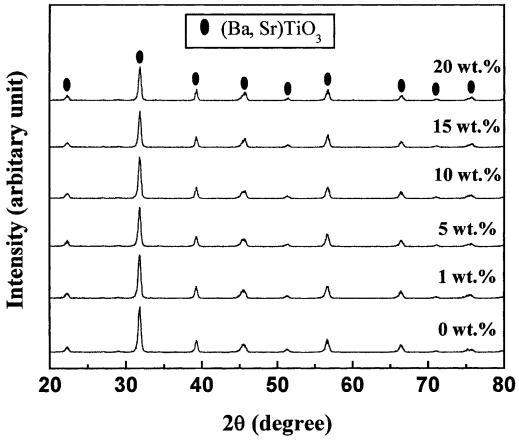

Fig. 4. XRD patterns measured at room temperature for n-$BaTiO_3$ ceramics containing various amount of PEG.

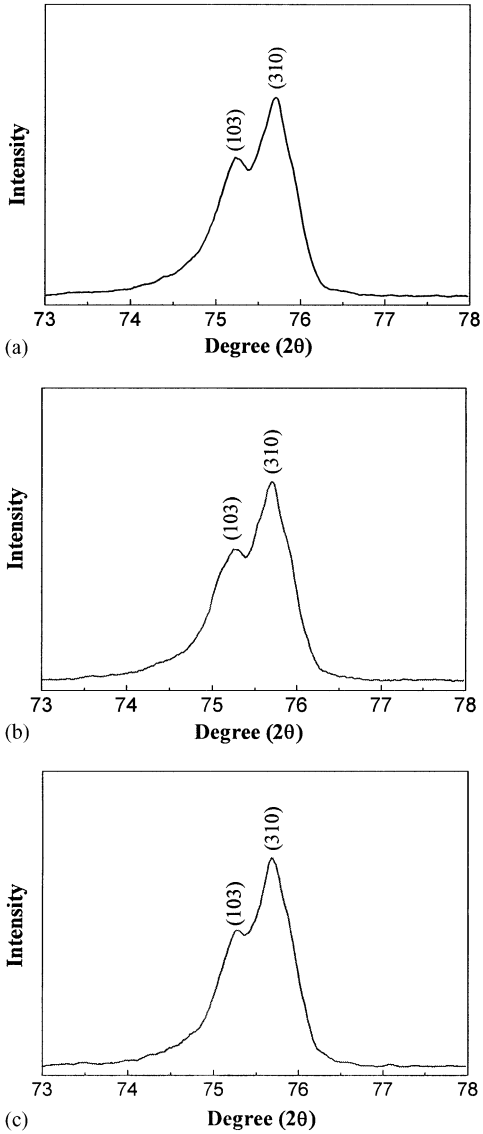

Fig. 5. XRD patterns measured at room temperature for n-$BaTiO_3$ ceramics containing (a) 0 wt.%, (b) 10 wt.% and (c) 20 wt.% of PEG.

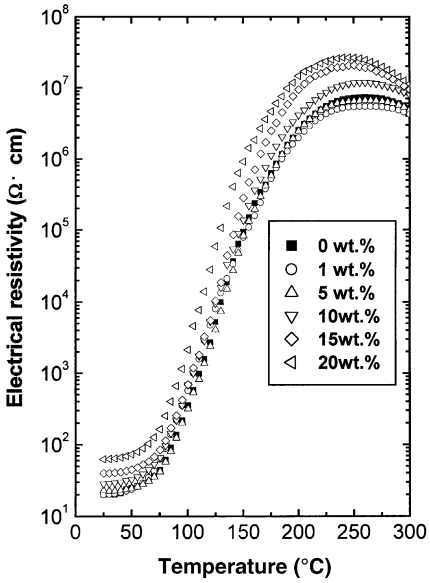

Fig. 6. Effect of temperature on the electrical resistivity of the *n*-$BaTiO_3$ ceramics containing various amount of PEG.

in the PTCR jump is due to the porosity and can be explained by the barrier model proposed by Heywang [11]. However, at room temperature the electrical resistivity of the *n*-$BaTiO_3$ ceramics containing PEG is higher than that of the *n*-$BaTiO_3$ ceramics without PEG, and increased with increasing PEG content. This can be explained by the fact that the increase of room temperature resistivity in the *n*-$BaTiO_3$ ceramics containing PEG results from increase of porosity and decrease of grain size with increasing PEG.

The complex impedance was measured to determine the electrical resistance of the grain boundaries. Fig. 7 shows the impedance spectra of the *n*-$BaTiO_3$ ceramics containing 20 wt.% PEG measured at 25 °C (a) and 150 °C (b). The electrical resistivity of grain boundaries at 25 °C ($\rho_{gb,25\,^\circ C}$) and 150 °C ($\rho_{gb,150\,^\circ C}$) are 6.24×10 and $9.11 \times 10^5\ \Omega$ cm, respectively. The electrical resistivity of grain boundaries for the *n*-$BaTiO_3$ ceramics containing various content of PEG is summarized in Table 1. The electrical resistivity of grain boundaries at above 150 °C could not be measured because the value is above the measuring limit ($10^6\ \Omega$ cm) of the

Table 1
Electrical resistivity of the grain boundaries (ρ_{gb}) for the various *n*-$BaTiO_3$ ceramics containing various amount of PEG

PEG content (wt.%)	Electrical resistivity		
	$\rho_{gb,25\,^\circ C}$ (Ω cm)	$\rho_{gb,150\,^\circ C}$ (Ω cm)	$\rho_{gb,150\,^\circ C}/\rho_{gb,25\,^\circ C}$
0	2.01×10	7.32×10^4	3.64×10^3
1	2.02×10	7.87×10^4	3.89×10^3
5	2.27×10	9.22×10^4	4.06×10^3
10	2.82×10	1.35×10^5	4.78×10^3
15	3.97×10	2.79×10^5	7.03×10^3
20	6.24×10	9.11×10^5	1.46×10^4

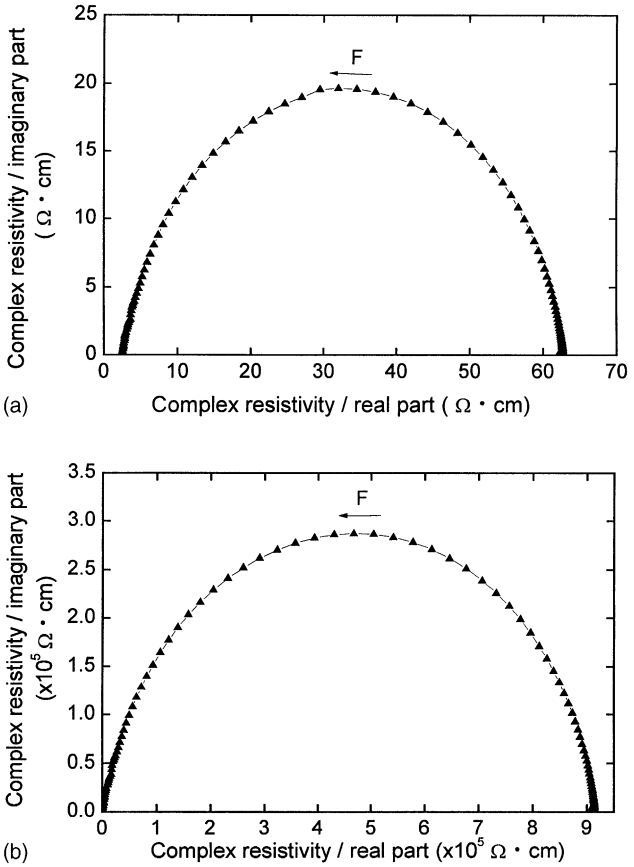

Fig. 7. Impedance spectra of the *n*-$BaTiO_3$ ceramics containing 20 wt.% PEG at 25 °C (a) and 150 °C (b). The arrow F indicates the direction of frequency increase from 5 Hz to 13 MHz.

analyzer used. The observed complex impedance indicates that the development of PTCR characteristic in the porous *n*-$BaTiO_3$ ceramics containing various content of PEG is related to grain boundaries, which basically equals to that in ordinary $BaTiO_3$ without PEG.

The porous *n*-$BaTiO_3$ ceramics can be successfully utilized for ceramic sensors (temperature, humidity and gas sensors) [19–21].

4. Conclusions

Porous $BaTiO_3$ (*n*-$BaTiO_3$) ceramics doped donor were prepared by adding polyethylene glycol (PEG) and the effects of PEG on the microstructure and PTCR characteristics of the porous *n*-$BaTiO_3$ ceramics have been investigated. The results obtained were as follows:

(1) From the DTA and TGA of the PEG, an endotherm was found at 60 °C, with strong exotherm at 262 °C, weight loss commenced at 165 °C and was virtually complete by 265 °C.
(2) With increasing PEG, the porosity increased and the grain size decreased. The porosity and grain size

of the *n*-$BaTiO_3$ ceramic containing 5 wt.% PEG is 10.4% and 6.3 μm, respectively, while it is 25.2% and 5.0 μm, respectively for the *n*-$BaTiO_3$ ceramic with 20 wt.% PEG.

(3) From the XRD results, the crystalline structure of *n*-$BaTiO_3$ ceramics was independent on the PEG content and the *n*-$BaTiO_3$ ceramics containing PEG showed the presence of (Ba, Sr)TiO_3 peaks only.

(4) The *n*-$BaTiO_3$ ceramics containing PEG showed higher PTCR characteristics than that of the *n*-$BaTiO_3$ ceramics without PEG.

(5) The development of PTCR characteristic in the porous *n*-$BaTiO_3$ ceramics containing various amount of PEG, in the same way as usual $BaTiO_3$ ceramics without PEG, is associated with grain boundaries.

(6) It is believed that newly prepared *n*-$BaTiO_3$ ceramics can be used for temperature, humidity and gas sensors.

Acknowledgements

This work was supported by Korea Research Foundation Grant (KRF-2001-005-E00009).

References

[1] H. Nagamoto, H. Kagotani, T. Okubo, Positive temperature coefficient resistivity in $Ba_{1-x}Sr_xPb_{1+y}O_{3-\delta}$ ceramics, J. Am. Ceram. Soc. 76 (1993) 2053–2058.

[2] H. Emoto, J. Hojo, Sintering and dielectric properties of $BaTiO_3$–Ni composite ceramics, J. Ceram. Soc. Jpn. 100 (1992) 555–559.

[3] I.C. Ho, Semiconducting barium titanate ceramics prepared by boron-containing liquid-phase sintering, J. Am. Ceram. Soc. 77 (1994) 829–832.

[4] I.C. Ho, H.L. Hsieh, Influence of potassium on preparation and performance of PTC resistors, J. Am. Ceram. Soc. 76 (1993) 2385–2388.

[5] H.F. Cheng, T.F. Lin, C.T. Hu, Effect of sintering aids on microstructures and PTCR characteristic of $(Sr_{0.2}Ba_{0.8})TiO_3$ ceramics, J. Am. Ceram. Soc. 76 (1993) 827–832.

[6] B.C. Lacourse, V.R.W. Amarakoon, Characterization of the firing schedule for positive temperature coefficient of resistance $BaTiO_3$, J. Am. Ceram. Soc. 78 (1995) 3352–3356.

[7] O. Saburi, Semiconducting bodies in the family of barium titanates, J. Am. Ceram. Soc. 44 (1961) 54–63.

[8] W. Heywang, Semiconducting barium titanate, J. Mater. Sci. 6 (1971) 1214–1226.

[9] G.H. Jonker, Some aspects of semiconducting barium titanate, Solid State Electron. 7 (1964) 895–903.

[10] J. Daniels, K.H. Hardtl, R. Wernike, The PTC effect of barium titanate, Philips Tech. Rev. 38 (1978/79) 73–82.

[11] W. Heywang, Resistivity anomaly in doped barium titanate, J. Am. Ceram. Soc. 47 (1964) 484–490.

[12] M. Kuwabara, Effect of microstructure on the PTCR effect in semiconducting barium titanate ceramics, J. Am. Ceram. Soc. 64 (1981) 639–644.

[13] M. Kuwabara, Influence of stoichiometry on the PTCR effect in porous barium titanate ceramics, J. Am. Ceram. Soc. 64 (1981) C170–C171.

[14] S.-M. Su, L.-Y. Zhang, H.-T. Sun, X. Yao, Preparation of porous $BaTiO_3$ PTC thermistors by adding graphite porosifiers, J. Am. Ceram. Soc. 77 (1994) 2154–2156.

[15] T.R. Shrout, D. Moffatt, W. Huebner, Composite PTCR thermistors utilizing conducting borides, silicides, and carbide powders, J. Mater. Sci. 26 (1991) 145–154.

[16] J.-G. Kim, W.-S. Cho, K. Park, PTCR characteristics in porous (Ba, Sr)TiO_3 ceramics produced by adding partially oxidized Ti powders, Mater. Sci. Eng. B 77 (2000) 255–260.

[17] T. Takahashi, Y. Nakano, N. Ichinose, Influence of reoxidation on PTC effect of porous $BaTiO_3$, J. Ceram. Soc. Jpn 98 (1990) 879–884.

[18] M. Kuwabara, Determination of the potential barrier height in barium titanate ceramics, Solid State Electron. 27 (1984) 929–935.

[19] T.J. Hwang, G.M. Choi, Humidity response characteristics of barium titanate, J. Am. Ceram. Soc. 76 (1993) 766–768.

[20] J. Wang, B. Xu, G. Liu, Y. Liu, F. Wu, X. Li, M. Zhao, Influence of doping on humidity sensing properties of nanocrystalline $BaTiO_3$, J. Mater. Sci. Lett. 17 (1998) 857–859.

[21] A.C. Caballero, M. Villegas, J.F. Fernandez, M. Viviani, M.T. Buscaglia, M. Leoni, Effect of humidity on the electrical response of porous $BaTiO_3$ ceramics, J. Mater. Sci. Lett. 18 (1999) 1297–1299.